Parallelization of WENO-Boltzmann schemes for kinetic descriptions of 2D semiconductor devices

J. M. Mantas[1], J. A. Carrillo[2], and Armando Majorana[3]

[1] Software Engineering Department - UGR, Granada, Spain. jmmantas@ugr.es
[2] ICREA - Dpt. Matemàtiques - UAB, Barcelona, Spain. carrillo@mat.uab.es
[3] Dip. Matematica e Informatica - UCT, Catania, Italy. majorana@dmi.unict.it

Summary. The parallelization of a direct WENO (Weighted Essentially Non-Oscillatory) solver for the 2D-spatial Boltzmann-Poisson system describing electron transport in Si-based semiconductor devices has been addressed.. . .

1 Introduction

The parallelization of a direct WENO (Weighted Essentially Non-Oscillatory) solver for the 2D-spatial Boltzmann-Poisson system describing electron transport in Si-based semiconductor devices has been addressed. A non-parabolic Kane energy-band and elastic acoustic and inelastic non-polar optical phonon operators have been used [CGMS03A] in the physical description of the electron transport in the device. This choice is by no means restrictive and more complicated band structures, including several valleys, and different scattering mechanisms, both intervalley and intravalley ones, can be included in a flexible way both in the numerical method and its parallelization [CCM04].

The numerical scheme which has been parallelized [CGMS03A, CGMS03B] uses a formulation of the Boltzmann-Poisson system in spherical coordinates for the wave vector space. After adimensionalization one is reduced to simulate the evolution in time t of the distribution function Φ in the five-dimensional space $(x, y, \omega, \mu, \phi)$, where x and y are the spatial coordinates, $\omega \geq 0$ is a dimensionless energy, $\mu \in [-1, 1]$ is the cosine of the angle with respect to the x-axis and $\phi \in [0, \pi]$ the azimuthal angle. The resulting Boltzmann equation reads

$$\frac{\partial \Phi}{\partial t} + \frac{\partial}{\partial x}(a_1 \Phi) + \frac{\partial}{\partial y}(a_2 \Phi) + \frac{\partial}{\partial \omega}(a_3 \Phi) + \frac{\partial}{\partial \mu}(a_4 \Phi) + \frac{\partial}{\partial \phi}(a_5 \Phi) = s(\omega) C(\Phi) \quad (1)$$

where the flux functions a_i and the Jacobian factor $s(w)$ can be seen in [CGMS03B]. The dimensionless collision operator $C(\Phi)$ is given by:

$$C\ (\Phi)(t,x,y,\omega,\mu,\phi) = \frac{1}{2\pi\, t^*}\int_0^{\pi}\int_{-1}^{1}[\beta\Phi(t,x,y,\omega,\mu',\phi')$$
$$+\ a\Phi(t,x,y,\omega+\alpha,\mu',\phi') + \Phi(t,x,y,\omega-\alpha,\mu',\phi')]d\phi' d\mu'$$
$$-\ \frac{1}{s(\omega)\, t^*}[\beta s(\omega) + as(\omega-\alpha) + s(\omega+\alpha)]\Phi(t,x,y,\omega,\mu,\phi)\,. \qquad (2)$$

where the constant parameters t^*, α, a and β depend on scattering mechanisms (see [CGMS03A] for a more detailed description).

Flux functions a_3, a_4 and a_5 depend on the electric field vector $\mathbf{E}$ which is computed self-consistently by solving the dimensionless Poisson equation in the 2D spatial domain

$$\Delta V = \epsilon\,[n(t,x,y) - N_D(x,y)]\,, \qquad (3)$$
$$\mathbf{E} = -\nabla V,$$

where ϵ is a dimensionless parameter, $N_D(x,y)$ the dimensionless doping profile, V the electric potential and $n(t,x,y)$ the electron density computed from Φ by

$$\int_0^{\pi}\int_0^{\infty}\int_{-1}^{1}\Phi\, d\mu\, d\omega\, d\phi. \qquad (4)$$

In the Boltzmann equation (1) the advection part is treated with a 5th order non-oscillatory finite difference WENO scheme [SHU98], the collision operator (2) is approximated by means of a quadrature formula and the time-dependent part is solved by an explicit Runge-Kutta method. Poisson's equation (3) is solved by an iterative standard SOR method computed at each Runge-Kutta step and a midpoint quadrature formula is used in (4) resulting in a charge-conservative method.

We refer to [CGMS03A, CGMS03B, CGMS04] for the complete description of the numerical method, a discussion of this particular choice of the numerical scheme and the comparison of the results with respect to Monte Carlo simulations. Let us briefly mention that high-gradient regions in macroscopic quantities, in particular: density, energy and mean velocity (see Fig. 2-3) clearly imply the existence of high-gradient regions both in physical space (x,y) and in velocity space (ω,μ,ϕ) for the unknown distribution function Φ (see also Fig. 5). In order to accurately approximate the derivatives in these regions, we use WENO reconstruction methods which are well fitted for this purpose [SHU98] and, moreover, they produce a high order approximation in smooth regions.

Results of the 1D case [CGMS03A] and of the 2D case [CGMS04] have been validated by comparing them to Monte Carlo methods, which give excellent results even with coarse grids. Moreover, in the 2D case Monte Carlo methods are not well apt for resolving almost empty regions in the device (close to the gate in a MESFET) while deterministic methods do. Therefore, these

deterministic results, although not competitive with Monte Carlo methods at the level of the execution time in 2D, should be used as *benchmarks* for Monte Carlo, hydrodynamic or drift-diffusion results. We refer to [CGMS04] for a more detailed discussion about WENO-Boltzmann versus Monte Carlo methods in 2D.

Other advantages of this method are the transient computation, the knowledge of the distribution function itself and not only of their moments as well as the absence of oscillations or numerical noise even close to regions between different boundary conditions. A drawback of the use of WENO schemes is that we are reduced to uniform grid sizes and almost rectangular type geometries. Nevertheless, these drawbacks can be overcome by using an interpolation between different uniform grid sizes as in [GCG04, SS03].

2 Parallelization and numerical results

The aim of this work has been to obtain efficient parallel implementations of this 2D-space solver for a PC cluster because this scheme demands a great deal of computing power. The parallelization is based on domain decomposition techniques. An analysis of the scheme reveals that the best choice to decompose the data structure of the solution Φ is by splitting only the physical space dimensions among the processors by following a 2D block-decomposition. For this purpose, a logical 2D grid of processors is automatically defined according to the actual spatial grid size and the available number of processors. In this way, only the flux terms for the physical space require communication among the processors. Moreover, an overlapping of communication and computation has been enabled to improve the performance in the computations of these fluxes. The rest of fluxes can be parallelized in a straightforward manner because remote communication is not required. This choice leads to a relatively low communication cost and involves an important reuse of the existing sequential code.

To solve the Poisson equation in order to compute the electric potential, a parallel red-black Successive Over-Relaxation (SOR) scheme is implemented following a data distribution which matches with the distribution followed by the WENO-Boltzmann solver. The time discretization is carried out by using a parallel implementation of a third-order low-Storage Runge-Kutta method [GS98] in order to save memory resources. An scalable message-passing implementation of the solver has been obtained for any number of processors by making use of the Message Passing Interface (MPI).

The parallel scheme has been applied to the simulation of a MESFET device (see Fig. 1) used in several works as a benchmark for testing electron transport solvers [JS94, CGMS03B, AMRS04]. The doping profile is given by $5 \times 10^{18} cm^{-3}$ in the n^+ regions and $10^{18} cm^{-3}$ in the n region.

Results for the density, the potential and the electric current field can be seen in Fig. 2-3 with an electric potential of $-0.8V$ at the gate and $1V$ at the

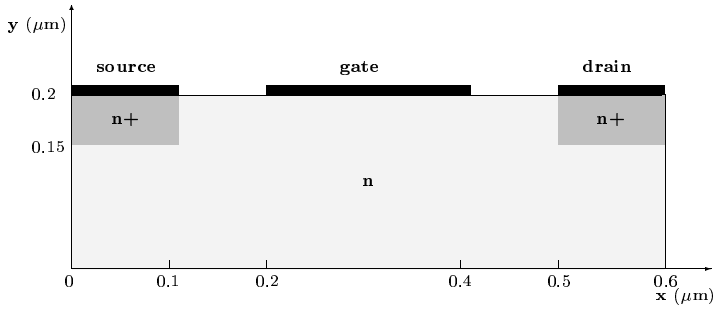

Fig. 1. Schematic representation of a 2D silicon MESFET device

drain with respect to the source. Several numerical experiments have been made on a cluster of 8 dual 2.5 Ghz AMD processors connected via a Gigabit ethernet switch. Numerical results for macroscopic quantities are shown at 5ps, where we use $48 \times 32 \times 102 \times 12 \times 12$ grid points for the $(x, y, \omega, \mu, \phi)$ domain.

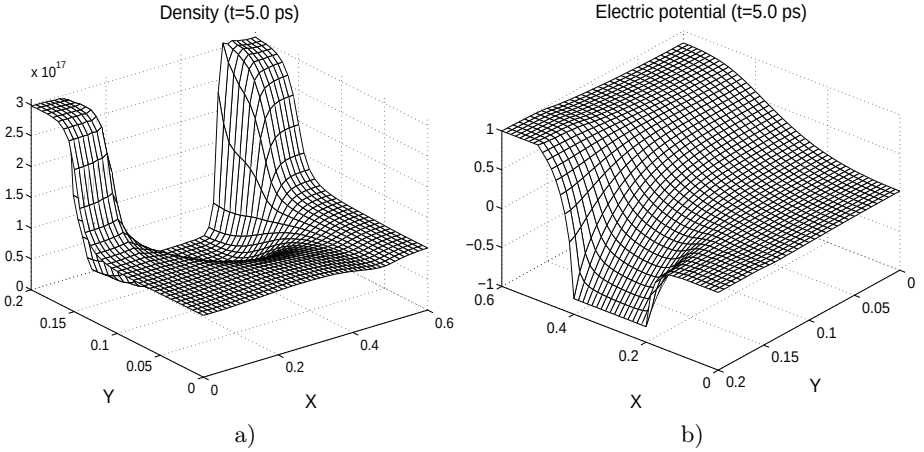

Fig. 2. a) Density (cm^{-3}) and b) potential (V) at 5 ps with a 48×32 spatial grid

Insulating boundaries are treated mimicking reflecting boundaries for the Boltzmann equation (1) and Neumann boundary conditions for the electric potential (3). As a result zero normal component to the insulating boundary of the electric current (see Fig. 3) is well resolved. Source and drain are Ohmic contacts and therefore we impose Dirichlet boundary conditions for the electric potential and inflow boundary conditions for the Boltzmann equation implying local neutrality. The gate is simulated as a Schottky contact and thus it should repel electrons. The gate region should have a very low density;

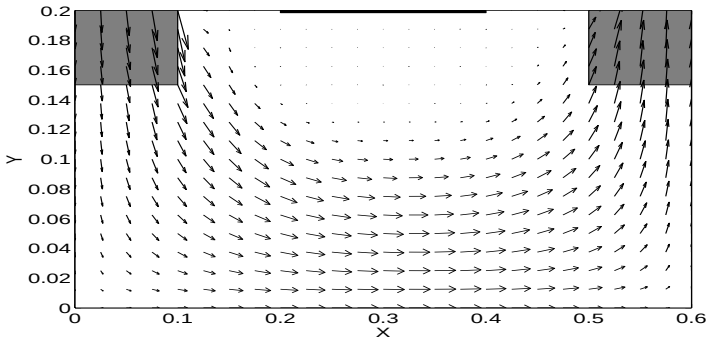

Fig. 3. Electric current field at 5 ps with a 48×32 spatial grid

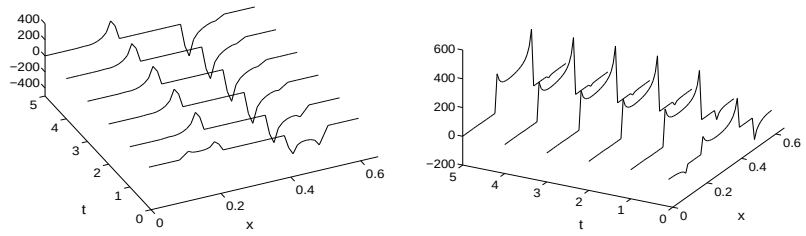

Fig. 4. Evolution of the Electric field at the top of the device in kV/cm: x-component (left) and y-component (right) with a 48×32 spatial grid

and the electrons may only leave the gate region to enter the device. As a consequence, the density at the gate is extremely small: more than 8 orders of magnitude lower than the doping profile. Therefore, we consider Dirichlet boundary conditions for the electric potential and zero charge density for the Boltzmann equation. We again refer to [CGMS04] for a detailed explanation of the implementation of the boundary conditions.

We clearly observe the appearance of singularities for the electric field at the points between insulating and contact boundary conditions at the top of the device. These singularities can be seen in figure 4 where the evolution of the electric field on the top of the device is plotted up to 5ps. They are not numerical artifacts and they do not disappear by grid refinement but on the contrary, they become larger in value resulting in a small CFL number for the time solver and therefore slowing the pace of the code. This is by no means a failure of the approach but a real success since it captures these singularities that appear even in drift-diffusion approximations [G93].

In Fig. 5 we observe the probability density function at three points of the device as a function of (w, μ) averaged over ϕ. We observe how the flow of electrons takes place since $\mu = 1$ is the direction of increasing x and $\mu = -1$ is the opposite.

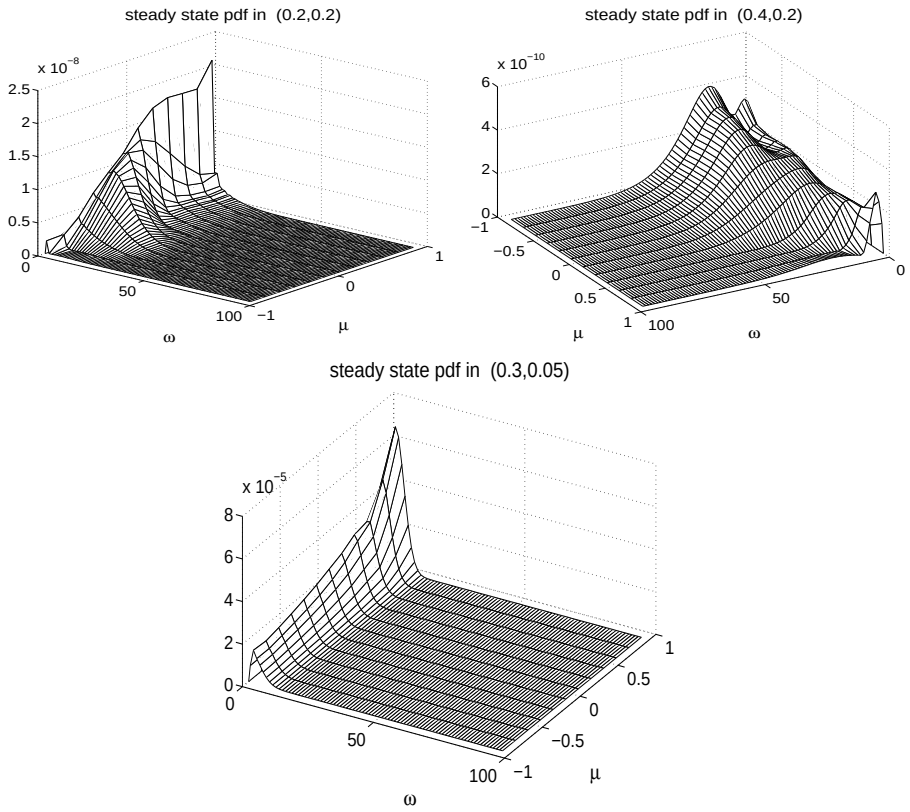

Fig. 5. Normalized PDF at 3 device points: top left figure at $(0.2, 0.2)$ (left corner of the gate), top right at $(0.4, 0.2)$ (right corner of the gate), bottom at $(0.3, 0.05)$

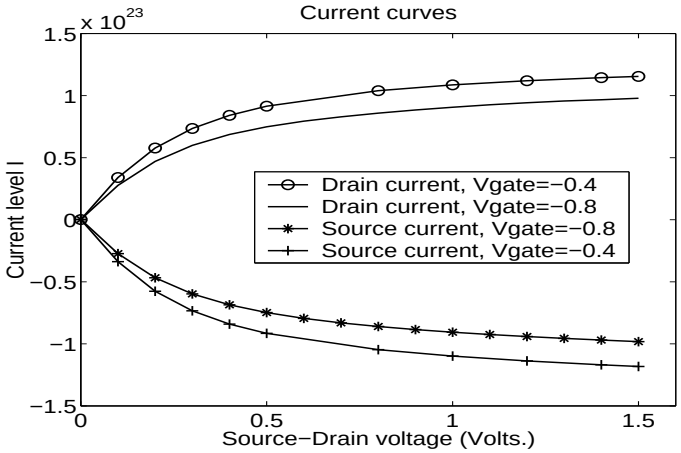

Fig. 6. Voltage-current curves at 5 ps with a 42×24 spatial grid

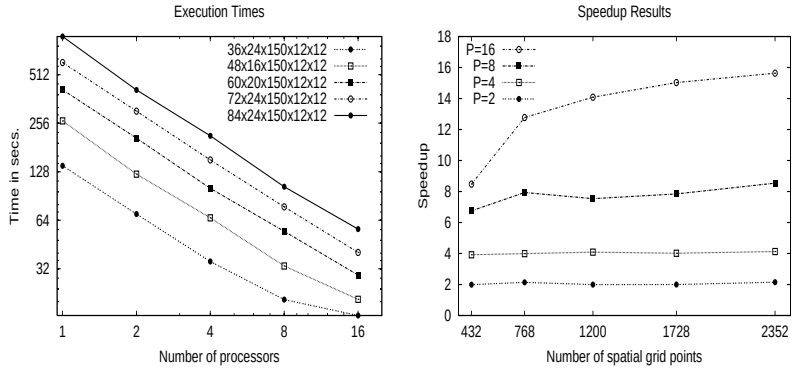

Fig. 7. Execution time results and speedup results for several spatial grid sizes

The efficient implementation of the scheme allows us to compute current-voltage characteristics for this device. The current-voltage characteristic curves when a voltage of -0.8 V and -0.4 V is applied at the gate are shown in Fig. 6. These results have been obtained by simulating the MESFET device at each of the drain voltage values corresponding to stars in Fig. 6 up to 5ps. Here, we use $42 \times 24 \times 80 \times 12 \times 12$ grid points for discretizing the $(x, y, \omega, \mu, \phi)$ domain. In this figure we show the computed current both at the drain and at the source since they should be equal up to a sign for the stationary solution and this is so up to 5 digits in all experiments performed.

Figure 7 shows execution times and speedup results obtained with several grid sizes and number of processors for the time integration of 0.01 picoseconds. The results show a good scalability in the range of processors [2,16] and a parallel efficiency close to 100 %.

3 Conclusions

A flexible parallelization of WENO-Boltzmann schemes for the kinetic description of realistic semiconductor devices has been performed. This method is flexible in band structure, scattering mechanisms and boundary conditions for the kinetic description and fairly flexible regarding the device geometry. Shown numerical results, in the particular case of a MESFET, reveal that these simulations although still computationally expensive and not competitive with Monte Carlo methods, provide useful benchmarks for all known solvers for charge particle transport in semiconductors and they are the most accurate simulations to date up to our knowledge.

Acknowledgements

The authors acknowledge support from the European IHP network HYKE "Hyperbolic and Kinetic Equations: Asymptotics, Numerics, Applications" HPRN-CT-

2002-00282. JM and JAC acknowledge partial support from DGI-MCYT/FEDER project BFM2002-01710. A part of the present work was carried out during a visit of the first author at the Dipartimento di Matematica e Informatica della Università di Catania. He is grateful to A. Majorana and G. Russo for their hospitality.

References

[AMRS04] Anile, A. M., Marrocco, A., Romano, V., Sellier, J.-M., Numerical simulation of 2D Silicon MESFET and MOSFET described by the MEP based energy-transport model with a mixed finite element scheme, preprint (2003).

[CGMS03A] Carrillo, J. A., Gamba, I., Majorana, A., Shu, C.-W. A WENO-solver for the transients of Boltzmann-Poisson system for semiconductor devices: performance and comparisons with Monte Carlo methods, Journal of Comp. Physics, **184**, 498–525 (2003).

[CGMS03B] Carrillo, J. A., Gamba, I., Majorana, A., Shu, C.-W. A direct solver for 2D non-stationary Boltzmann-Poisson systems for semiconductor devices: a MESFET simulation by WENO-Boltzmann schemes, Journal of Comp. Electronics, **2**, 375–380 (2003).

[CCM04] Cáceres, M. J., Carrillo, J. A., Majorana, A., Deterministic simulation of the Boltzmann-Poisson system in GaAs-based semiconductors, HYKE preprint HYKE2004-111, `www.hyke.org`, (2004).

[CGMS04] Carrillo, J. A., Gamba, I., Majorana, A., Shu, C.-W., 2D Device simulations by WENO finite differences approximations of the Boltzmann-Poisson system for semiconductors, work in preparation, (2004).

[G93] Gamba, I., Asymptotic behavior at the boundary of a semiconductor device in two space dimensions, Ann. di Mat. Pura App. (IV) Vol. CLXIII, 43-91, (1993).

[GCG04] González-Rodelas, P., Carrillo, J. A., Gámiz, F. Deterministic Numerical Simulation of 1d kinetic descriptions of Bipolar Electron Devices, to appear in proceedings of the 5th International Workshop in Scientific Computing in Electrical Engineering (2004).

[GS98] Gottlieb, S., Shu, C.-W., Total variation diminishing Runge-Kutta schemes, Math. Comp., **67**, 73-85 (1998).

[JS94] Jerome, J.W. and and Shu, C.-W., "Energy models for one-carrier transport in semiconductor devices", in IMA Volumes in Mathematics and Its Applications, v59, W. Coughran, J. Cole, P. Lloyd and J. White, editors, Springer-Verlag, 1994, pp.185-207.

[SHU98] Shu, C.-W. Essentially non-oscillatory and weighted essentially non-oscillatory schemes for hyperbolic conservation laws, Lecture Notes in Mathematics **1697**, 325-432 (1998).

[SS03] Sebastian, K., Shu, C.-W., Multidomain WENO finite difference method with interpolation at subdomain interfaces, J. Scientific Computing, **19**, 405-438 (2003).